Improved Estimation of Proxy Sea Surface Temperature in the Arctic

VIVA BANZON[a]

NOAA/NESDIS/NCEI, Asheville, North Carolina

THOMAS M. SMITH

NOAA/NESDIS/STAR, College Park, Maryland

MICHAEL STEELE

Polar Science Center, Applied Physics Laboratory, University of Washington, Seattle, Washington

BOYIN HUANG AND HUAI-MIN ZHANG

NOAA/NESDIS/NCEI, Asheville, North Carolina

(Manuscript received 24 October 2019, in final form 12 December 2019)

ABSTRACT

Arctic sea surface temperatures (SSTs) are estimated mostly from satellite sea ice concentration (SIC) estimates. In regions with sea ice the SST is the temperature of open water or of the water under the ice. A number of different proxy SST estimates based on SIC have been developed. In recent years more Arctic quality-control buoy SSTs have become available, allowing better validation of different estimates and the development of improved proxy estimates. Here proxy SSTs from different approaches are evaluated and an improved proxy SST method is shown. The improved proxy SSTs were tested in an SST analysis, and showed reduced bias and random errors compared to the Arctic buoy SSTs. Almost all reduction in errors is in the warm melt season. In the cold season the SIC is typically high and all estimates tend to have low errors. The improved method will be incorporated into an operational SST analysis.

1. Introduction

Temperature is a key indicator of climate change in the Arctic. However, sea surface temperature (SST) observations in this region are limited, whether from satellite or in situ platforms. A common practice is to generate simulated, or proxy SST based on sea ice concentrations (SIC), for which there is good coverage in the Arctic from satellite observations. The SST in ice-covered regions is defined as the seawater surface temperature in open-water areas for partial ice-covered regions. In fully ice-covered regions it is the seawater temperature just below the ice. An example of SST simulated from NASA Team SIC is shown in Fig. 1a. The other panels show SST estimates from satellites and buoys for the same day. The observed SSTs are much sparser but roughly consistent with the estimates from SIC in areas near the ice. Different SIC estimates are discussed in section 2. The SIC is given as the fraction of a sampled region covered by sea ice, from 0 to 1. The SST simulated from the SIC can be used as an input for an SST analysis, that is, a gap-filled SST map used in a wide range of applications such as weather prediction, climate studies, and ecological modeling.

There are many methods for converting sea ice concentration to SST. Examination of the most commonly used level 4 (L4) products from GHRSST indicates four main approaches. The simplest approach is to set the SST to the freezing point of seawater (approximately −1.8°C). Chin et al. (2017) set SST to the freezing value north of 88°N regardless of ice concentration, to compensate for the lack of data near the

Denotes content that is immediately available upon publication as open access.

[a] Retired.

Corresponding author: Thomas M. Smith, tom.smith@noaa.gov

DOI: 10.1175/JTECH-D-19-0177.1

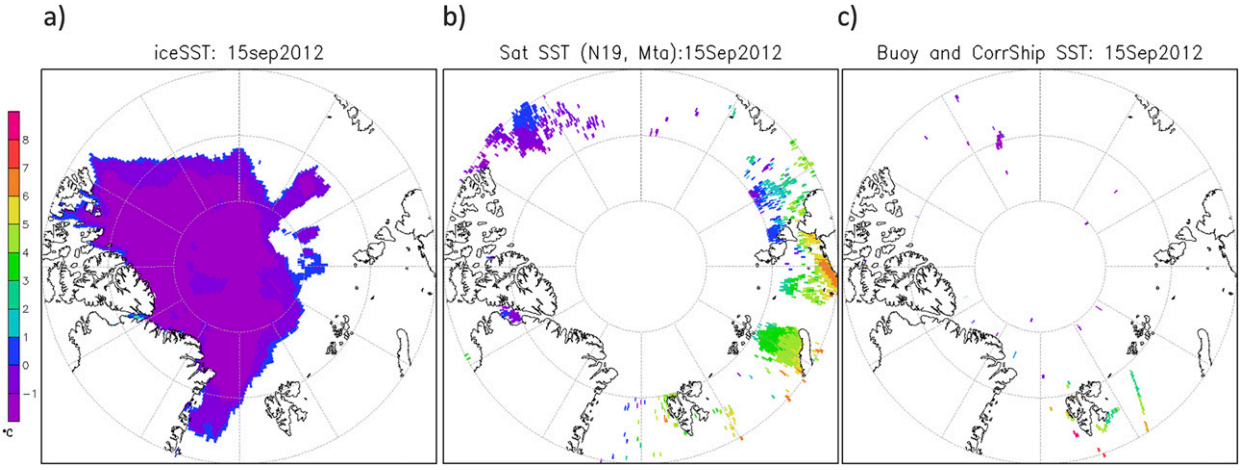

FIG. 1. Maps of SST inputs: (a) ice SST based on NASA Team SIC and the current OISST methods; (b) satellite SSTs (combined day and night from *MetOp-A* and *NOAA-19*); and (c) in situ SSTs. All are daily estimates for 15 Sep 2012.

North Pole, and everywhere else where SIC $>$ 0.3 to deal with the ice margins. Donlon et al. (2012) compute a first guess in ice zones that assigns a background SST value of −1.8°C where SIC $>$ 0.5 and relaxes the anomaly from the previous time step toward that background value. The forcing toward the background value is dependent on the SIC, with modest forcing for SIC at 0.5 and much stronger forcing for SIC at 1.0.

A second approach is used by Brasnett and Surcel Colan (2016). In most cases when the sea ice concentration is at least 0.6 they estimate the SST as −1.8°C. They adjust that estimate when an analysis of surface air temperature is above 0°C and the ice concentration is between 0.6 and 0.9. In that case they assume that meltwater is present and they set the SST to 0°C. In their analysis of the Arctic they assign a large error estimate of the proxy SST estimated this way.

A third approach, used in the Real-Time Global (RTG) analysis, derives the surface freezing temperature from Millero's formula (see Fofonoff and Millard 1983, and references therein) and the Levitus (1982) salinity climatology (Thiebaux, J.E., 2003; and https://polar.ncep.noaa.gov/sst/rtg_high_res/description.shtml). The annual Levitus (1982) salinity is needed since seasonal estimates for that climatology are too sparsely sampled to describe the entire Arctic. The RTG estimate is used by Maturi et al. (2017) for the Arctic. Surface salinity has large spatial variation over the Arctic Ocean with relatively low values, about 20 psu, on some shelves. Within the Atlantic inflow from the Nordic seas salinity is much higher, around 34–35 psu (Zweng et al. 2013). This gives surface freezing temperatures of between −1.08° and −1.87°C (Fofonoff and Millard 1983). There is also strong seasonal change in surface salinity, which is not accounted for when using the annual mean. Thus, using a salinity climatology improves the surface freezing temperature estimate compared to holding it constant at −1.8°C, and a seasonal climatology is better than an annual climatology. Improvements can be increased by use of an updated climatology that better reflects recent changes in Arctic salinity. With the typical Arctic salinity, the rate of change of surface freezing temperature with salinity is roughly $-0.06°\text{C psu}^{-1}$. The Measuring the Upper Layer Temperature of the Polar Oceans (UpTempO) buoy accuracy is 0.1°C, so a 2-psu change could cause detectible errors. Since the regional and seasonal salinity changes could cause Arctic SST changes that are important to some users, it is useful to minimize the errors associated with those changes.

Regression formulas have also been used to relate satellite SST estimates to SIC. Regressions have taken various forms, including linear (Reynolds et al. 2007, hereafter REA07), quadratic (Reynolds et al. 2002; Rayner et al. 2003), or cubic (Hurrell et al. 2008). REA07 reasoned that a bilinear equation is sufficient to approximate the quadratic relation, and can be further simplified into a linear equation if applied only where SIC $>$ 0.5. With the regression approach, the proxy SST value is set to a minimum constant temperature (−1.8°C for oceans, 0.0°C for large lakes) when the ice concentration is above a certain threshold value. When the ice concentration is less than the threshold value, the regression formula is then used. The regressions vary temporally and geographically, with the boundaries varying by authors.

There are valid arguments why each of these four approaches may work. As noted in Reynolds et al. (2002; REA07), the regressions are fit to the best data available at the time of their development, although there are now

some better Arctic SST estimates. The RTG estimate is based on a physical limit, the freezing temperature of seawater. But there is now an improved monthly salinity climatology for computing the freezing temperature so it could be improved.

Until recently there was not enough quality-controlled in situ data in the Arctic to evaluate the various approaches or to develop better methods. Quality control is needed to remove suspect or unrealistic SSTs, which can occur when buoys are frozen out of the water and exposed to air. These problems are here addressed using data from the UpTempO project, available in a raw and quality-controlled version. Castro et al. (2016) used the UpTempO to show large differences (sometimes in excess of 2°C) among the analyzed SST values in the Beaufort Sea. These differences may be due to the proxy SST estimation or from how the proxy SST is analyzed.

The focus of this study is on the proxy SST estimation methods using an expanded UpTempO dataset. First, we verify the relationship between SST and ice, which is the basic assumption of the ice-to-SST conversion. Next, we generate proxy SST using the four main methodologies and validate them using the in situ data. Finally, we investigate ways to improve and implement the best method, for inclusion in the NOAA 0.25° daily Optimum Interpolation SST (OISST; described by REA07) analysis.

In the following sections, first the datasets used are described. That is followed by a section that examines the relation between SIC and SST and the evaluation of the four proxy methods discussed above. The adaptation of the method for use in OISST is then discussed, followed by a brief summary and conclusions section.

2. Data and methods

This study uses the NASA Team SIC dataset at 25-km resolution (also identified as NSIDC-0051; Cavalieri et al. 1996, 1999). Available from 1978, it is the ice dataset used for computing proxy SSTs in long runs of OISST and has been used for other long-term SST analyses (e.g., Rayner et al. 2003). The NSIDC-0051 SIC is available with about 1 year of latency. This particular SIC dataset had been used for long OISST analyses in the past and therefore was used here. There may now be better long-record SIC datasets, and we hope to evaluate them for possible use in future improvements to the analysis. That could potentially give additional improvements, but the basic improvements shown in the new proxy SST estimates are not expected to change.

The NCEP ice is used for operational daily OISST updates. The NCEP SIC is on a 0.5° grid in GRIB format. Data for the most recent 3 days are available online (ftp://ftpprd.ncep.noaa.gov/data/nccf/com/omb/prod/), and older data are in monthly or yearly files (which can be obtained from ftp://polar.ncep.noaa.gov/cdas/archive/). The 0.5° data are linearly interpolated onto the OISST 0.25° grid. In addition, some testing was done using a higher-resolution version of the NCEP SIC averaged to the 0.25° grid (downloaded from ftp://polar.ncep.noaa.gov/cdas/archive/). On the 0.25° grid there is little difference between results from the two NCEP SIC analyses. Some further details of the NCEP product are given by Grumbine (2014).

The buoy SSTs are level 2 quality-controlled UpTempO data (Steele et al. 2018; see also similar datasets for other years at the Arctic Data Center and at http://psc.apl.washington.edu/UpTempO/). The shallowest temperature in profile is identified by first wet thermistor (FWT) indicator. The data are most consistently reliable from 2012 onward. UpTempO buoys have been described in Castro et al. (2016). With regard to level 2 data, they have been quality controlled relative to raw level 1 data via (i) bias and drift checks against nearby in situ temperature profile data (when available) and subtraction of long-term trends in the deepest temperature and pressure sensors, (ii) range checks for unphysical values, and (iii) outliers, dead sensors, and other miscellaneous noise. Most buoys have been deployed in summertime in open water in the Beaufort Sea, with some in the northern Chukchi and Laptev Seas; they subsequently freeze into the pack ice and drift throughout the Arctic Ocean.

3. Filling the pole-hole gap

The NASA Team SICs are retrieved from microwave observations from a series of satellites. Due to the satellite inclination, there is an observational data gap around the North Pole [referred to as the pole-hole gap (PHG); see Fig. 2]. The size of the PHG is satellite dependent (Table 1). There are similar gaps around the South Pole, but because they are over the Antarctic continent, they do not affect sea ice estimates. Because our intent is to use the sea ice concentration to generate the proxy SST, it is important to fill the Arctic PHG.

The PHG may be filled using bilinear interpolation as is done in the OISST analysis (REA07) and in the Ocean and Sea Ice Satellite Application Facility (OSI SAF) ice (Lavelle et al. 2017). In REA07, the bilinear interpolation is done after the ice data have been remapped to a rectangular grid. Strong and Golden (2016, hereafter SG16) developed a method that proved superior to the bilinear method and is done using polar projected data. To evaluate the SG16 method the SIC data for 2012

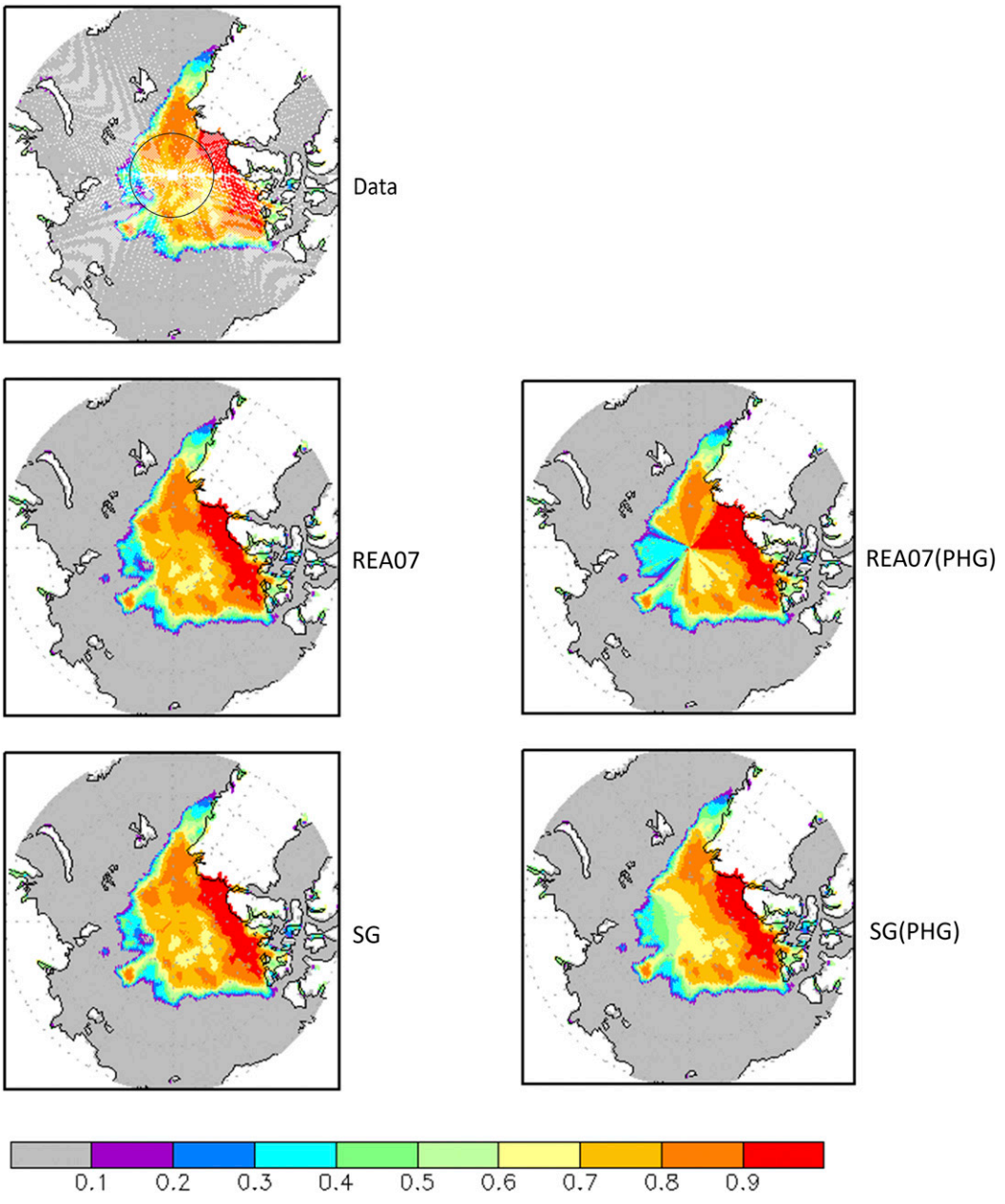

FIG. 2. (left) NASA Team sea ice concentrations for 15 Sep 2012 with a pole-hole radius of (top) 94 km, (middle) REA07 filled, and (bottom) SG16 filled. (right) Simulated 611-km-radius hole (middle) REA07 filled and (bottom) SG16 filled. The black circle in the top-left panel is approximately the larger PHG region where data are discarded for testing.

were used, when SIC reached a long-term minimum. From 2008 onward, the PHG is small, making it possible to conduct an experiment by withholding data to simulate conditions for when the PHG is much larger. The focus was on September when monthly melting tends to be greatest, making the most variation in ice concentrations. The high variation makes filling the pole hole particularly challenging. Here we test the SG16 method and compare it with the bilinear method of REA07. C. Strong and K. Golden (2018, personal communications) provided filled values using their method for September 2012 using all data and for a test of an extended PHG that omitted data north of 85°N. Note that in Fig. 2, 85°N is indicated by the black circle in the top-left panel from the latitude just north of Greenland. The month used for the test, September 2012, is a month with particularly

TABLE 1. Satellite pole-hole masks and sizes for different time periods (from http://nsidc.org/data/NSIDC-0051).

Pole-hole mask name	Pole-hole area (million km^2)	Pole-hole radius (km)	Lat (°N)	Dates used
SSMIS pole-hole mask	0.029	94	89.18	January 2008–present
SSM/I pole-hole mask	0.31	311	87.2	July 1987–December 2007
SMMR pole-hole mask	1.19	611	84.5	November 1978–June 1987

low Arctic sea ice, making this a severe test of the interpolation methods.

Using the full data and the infilling results using the two methodologies give similar results when the PHG is small. For example, for 15 September 2012 both the REA07 and SG16 methods give similar results (Fig. 2, left panels) and comparisons are similar over the entire month. For times with a small PHG either method can be used. The challenge is to fill for periods when the PHG is relatively large. When data are withheld north of 85°N the REA07 method produces a wedge-shaped pattern, while the SG16 gives a more natural pattern as seen in the 15 September example (Fig. 2, right panels). Over all days of the month the root-mean-square error (RMSE) relative to the full data is higher for the REA07 method (0.141) compared to the SG16 method (0.100). Based on these tests we conclude that the SG16 method should be used for PHG filling for the period before 2008, and is less critical after 2008. The ice dataset used here uses the SG16 method.

4. Proxy SST computations

First, the 7-day median of the SIC was computed to reduce day-to-day noise and to fill short temporal gaps. The median ice was converted to pseudo SSTs using the four approaches previously discussed, although we do not strictly follow what others have done. In particular, many analyses tend to estimate the pseudo SST only where SIC > 0.5 because the estimate is less reliable where there is more open water. Here the computations are done for the full range of nonzero ice concentrations to see if the threshold of 0.5 is justified. To summarize, the four estimates of SST from SIC tested are 1) set SST to a constant −1.8°C (FrzPtSW), 2) set SST to −1.8°C unless air temperature > 0°C and then set SST to 0°C (AirTemp), 3) set SST to the freezing-temperature climatology based on the salinity climatology (FrzPtClm), and 4) a linear fit to estimate SST from SIC developed using satellite SST estimates (LinearFit). We test for all SIC > 0 to show the accuracy of the estimates at SIC below the level when the estimates are normally used for SST analysis. Only when we compute the OISST do we restrict the concentration at which we use the proxy SST. These tests are intended to evaluate the relative accuracy of the different estimates of SST from SIC. Biases may still exist, especially in the warm season when the NASA Team algorithm may interpret melt ponds as open water. Comparisons to the available buoy observations indicate the relative accuracy of the different methods.

For the FrzPtClm approach, a monthly sea surface salinity climatology used is from the *World Ocean Atlas* (*WOA*; Zweng et al. 2013) from 1955 to 2012. The computation of sea surface freezing temperature as a function of salinity follows Fofonoff and Millard (1983). The LinearFit method produces proxy SSTs by applying the linear-fit equation developed by REA07. They used a 10-yr training period of satellite SST and SIC to develop regressions and performed a validation using a subsequent 10-yr period. They found that a linear fit performed better than a quadratic fit that had been used previously.

5. Overall and seasonal results

A plot of the Arctic UpTempO buoy SSTs against the NASA Team median ice concentrations suggest a relationship, although for some months a constant SST may be sufficient (Fig. 3). From January to May, most buoys are located in areas that are ice covered (SIC > 0.8) and in situ temperatures are close to freezing (−1.5° to −1.9°C). In the warmer months (July to October), the buoy data represent a wide range of ice concentrations. Individual months show a roughly linear pattern in June–July that appears to become more bilinear in August–September. Later in the cool season the shape flattens.

Based on the result with the UpTempO buoys, one might expect the LinearFit to produce reasonable SST estimates. However, a plot of the Arctic LinearFit proxy SSTs against buoy observations shows that the simulated temperatures are often too warm (Fig. 4, left panel). This is likely because the regression was based on satellite SSTs, which are rare in the Arctic and concentrated around the outer edge of the basin (Fig. 1). The warm biases in the LinearFit may also be influenced by warm season melt ponds on the surface of the ice, which may be warmer than open-ocean SST.

Using the freezing temperature gives good agreement at lower Arctic buoy temperatures, but with

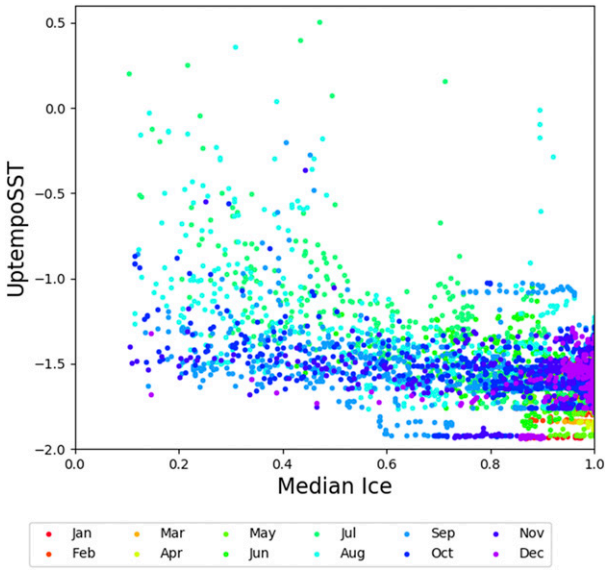

FIG. 3. Arctic UpTempO SST vs median sea ice concentration for all months. Individual months are indicated by the colors.

higher buoy temperatures that estimate tends to be too cool (Fig. 4, right panel). One possible reason for the cool bias in the warm season may be that a greater fraction of open sea in a grid square can lead to less reflectance and more warming of the open water. In addition, variations in winds and differences between the climatology and the actual salinity can also contribute to that bias.

To evaluate the proxy SST estimates against the buoy estimates we consider the RMSE, the bias, and the standard deviation of the error (SDE). Note that the squares of the bias and SDE components equal the square of the total RMSE: $\text{RMSE}^2 = \text{Bias}^2 + \text{SDE}^2$. Therefore, we can look at RMSE in terms of the contribution of the bias and SDE (Fig. 5).

The freezing-point climatology (FrzPtClm) estimate had the lowest RMSE along the full range of ice concentrations, with consistently lower bias than the estimate that holds the freezing temperature constant (FrzPtSW), which has second lowest RMSE. For SIC < 0.5, estimates adjusted using the air temperature above 0°C (AirTemp) had similar RMSE as the FrzPtSW, but the RMSE was higher for SIC > 0.5, mostly due to SDE. The UpTempO has quality control to avoid reporting melt-pond temperatures (i.e., the temperature of ponds on the surface of the ice that are separated from the ocean), so we can expect it to have larger differences anywhere the SST is set to 0°C. This comparison suggests that setting the SST to 0°C where the air temperature is above that temperature may increase noise in the estimate for high SIC. The linear-fit estimate gives the largest overall error, almost entirely from its much larger bias.

In individual months there can be slight differences from the all-month results discussed here, but the overall conclusions are not changed. Since the largest errors are associated with lower SIC values, which occur mostly in the warm season, the results discussed here are most representative of the warm season. In the cool season, the SIC used for comparisons tend to be high in most regions, giving smaller errors for all methods. That is because UpTempO is deployed mostly in the high Arctic Ocean Basin, which is completely covered by ice

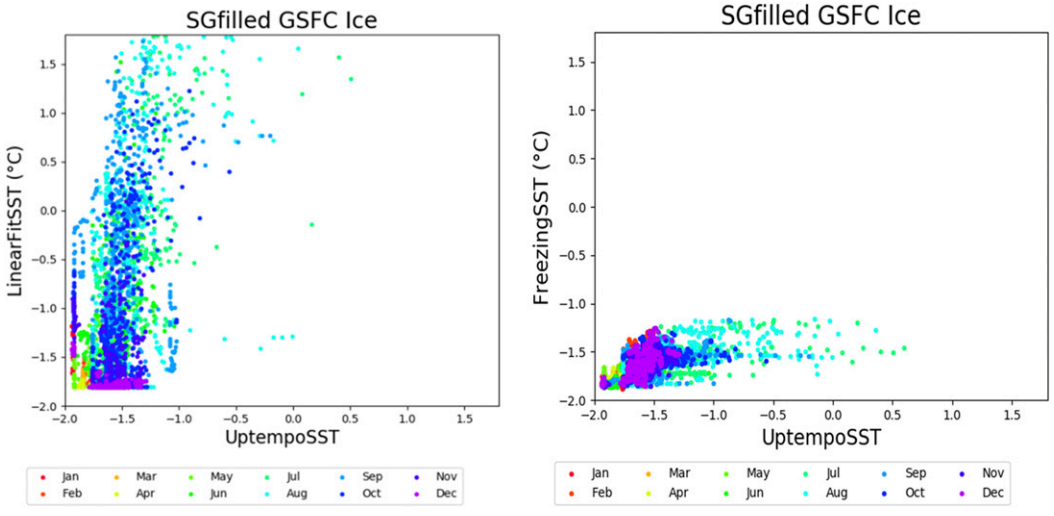

FIG. 4. UpTempO SST vs proxy SST estimates based on SIC from (left) the LinearFit and (right) the freezing temperature of seawater estimate for observations with SIC > 0.

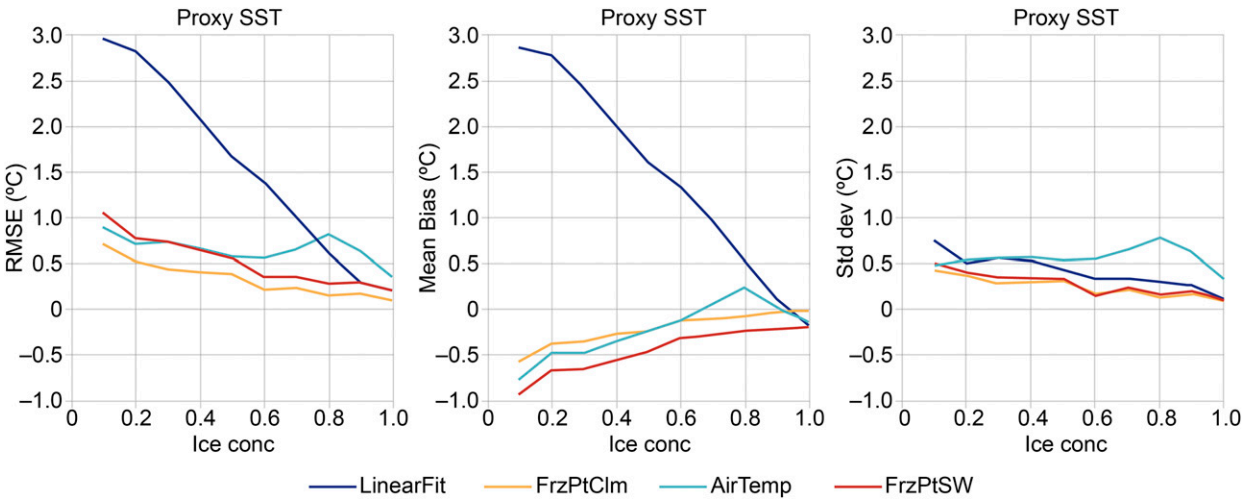

FIG. 5. Proxy SST (left) error and (center),(right) error components for the linear fit (LinearFit; dark-blue line), using the freezing-point climatology (FrzPtClm; orange line), using a constant freezing point of seawater (FrzPtSW; red line), and adjusting the freezing point of seawater using air temperature to set SST to 0°C when the air temperature is above 0°C (AirTemp; light-blue line).

in winter. There are low SIC areas in winter, but they tend to be south of where the buoys are deployed.

6. Improving the climatological freezing-point method

Of the four estimates tested, the climatological freezing-point method gives the lowest overall RMSE compared to the available quality-controlled buoy observations. However, the bias in that method at low SIC suggests that it may be improved by an adjustment factor dependent on the SIC.

If T_f is the daily climatological freezing temperature then the freezing-point method can be adjusted using the median SIC,

$$T_s(\mathrm{SIC}) = T_f + C(1 - \mathrm{SIC}) \quad \text{for} \quad 0 < \mathrm{SIC} \leq 1.$$

The constant C is assigned from examination of the bias of the climatology freezing-point estimates as a function of ice concentrations. For the NCEP SIC the constant is about 1.2, while for the NASA Team SIC it is about 0.4. For no adjustments the constant would be set to 0.

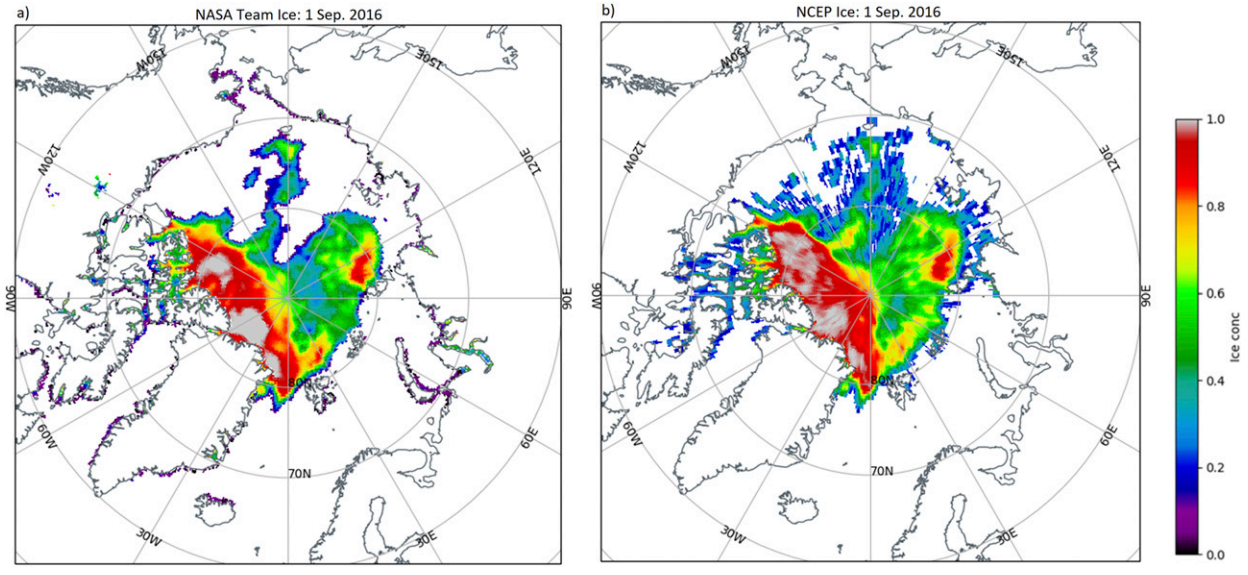

FIG. 6. Ice concentrations for 1 Sep 2016 plotted in polar projection for the Arctic: (a) NASA Team ice data; (b) NCEP 0.5° ice data interpolated to a 0.25° grid as used in the operational production.

By lowering the bias of the climatological freezing-point estimates, adjustments provide lower overall errors for the estimates and can improve the Arctic OISST estimates. The reduced RMSE and bias indicate that the freezing-point approach may be used everywhere there is ice, while the linear fit is best applied only where SIC > 0.5 because of its high RMSE at low concentrations.

The adjustment accounts for warming in regions with partial ice cover. In the cool season, when warming is less likely, most areas have higher ice cover so there may be little advantage to having a seasonal-dependent adjustment. For that reason, the adjustment was not tested for the cool season. Further study is needed to more clearly show if there is seasonal dependence.

The different adjustment constants are used for the different SIC estimates because of how those estimates are produced. At high SIC values the two estimates are similar, but the NCEP SIC estimate tends to have more ice at low SIC values (Fig. 6). These differences can matter since the NCEP SIC is used for operational OISST analysis because of its near-real-time availability, while the NASA Team SIC has a longer time delay. However, using the appropriate adjustment constants minimizes the impact of the choice of SIC analysis on the proxy SST estimates.

Validation against the Arctic buoys is done for the Arctic OISST results computed using several SIC to SST estimates. The OISST runs include one using the linear fit for SIC > 0.5, which is the method presently used for operational OISST. In addition, there are OISST runs using the climatological freezing-point estimate when SIC > 0.5, using both the climatological freezing-point estimate when SIC > 0 and the adjusted climatological freezing-point estimate when SIC > 0. Errors are computed as a function of SIC (Fig. 7). All freezing-point estimates give lower OISST errors than the linear-fit estimate, especially at low SIC. In addition, there is a clear advantage to using the climatological freezing-point estimates for lower ice concentrations, and the adjustment reduces the bias in the freezing-point estimate at low concentrations.

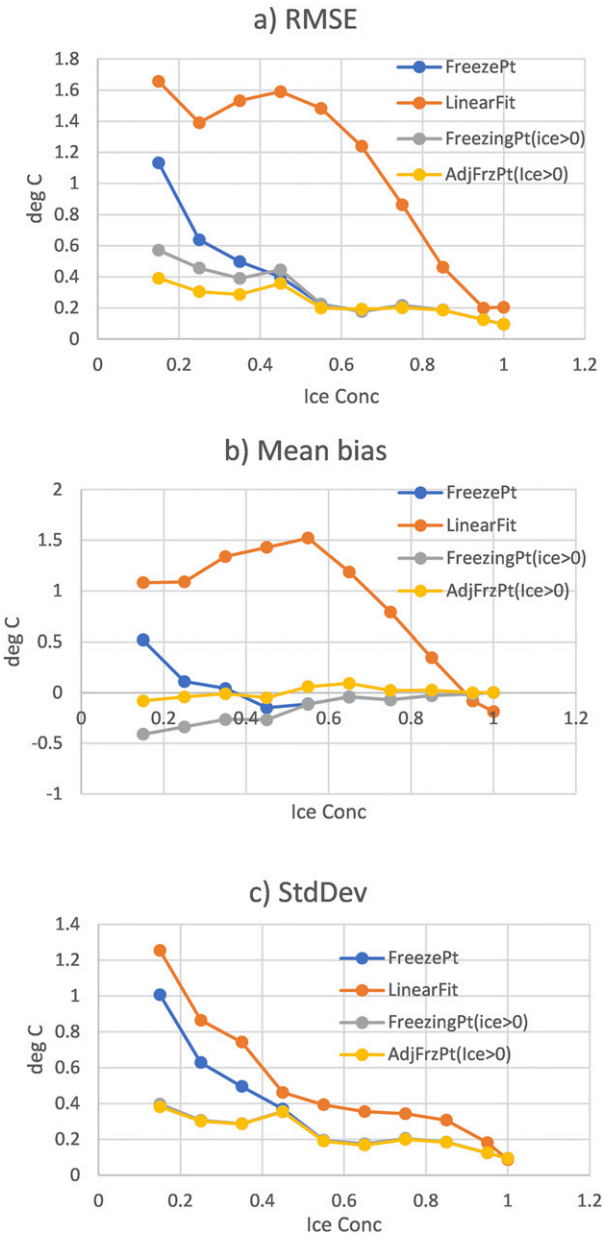

FIG. 7. OISST errors as a function of ice concentration using different sea ice–to-SST estimates: (a) RMSE; (b) bias; (c) error standard deviation. FreezePt is the proxy SST set to the climatological freezing point where 0.5 ≤ SIC, LinearFit is the proxy SST computed using an ice-to-SST equation where 0.5 ≤ SIC, FreezingPt(ice>0) is the proxy SST set to the climatological freezing point where 0 < SIC, and AdjFrzPt(ice>0) is the proxy SST set to the climatological freezing point where 0 < SIC and adjusted as described.

7. Summary and conclusions

When the REA07 OISST analysis was developed there were insufficient Arctic in situ data for developing sea ice–to-SST estimates, so satellite data were used and the SST was estimated as a linear function of sea ice concentration (SIC) for SIC > 0.5. More recently, quality-controlled in situ SST estimates for the Arctic have become available, allowing the development of improved SST estimates as a function of SIC. This note documents several estimates of SST as a function of SIC and the influence of the different estimates on the Arctic OISST. We show that Arctic OISST errors can be reduced by using an improved sea ice–to-SST estimate based on the climatological freezing temperature of surface seawater, with an adjustment as a function of SIC.

This improvement will be incorporated into an updated operational OISST.

Acknowledgments. We thank C. Strong and K. Golden for providing output of the test of their method using recent data and a simulated pole hole. M. Steele was supported by grants from ONR N00014-17-1-2545, NSF OPP-1751363, PLR 1603266, and NASA NNX16AK43G, 80NSSC18K0837. The contents of this paper are solely the opinions of the authors and do not constitute a statement of policy, decision, or position on behalf of NOAA or the U.S. Government.

REFERENCES

Brasnett, B., and D. Surcel Colan, 2016: Assimilating retrievals of sea surface temperature from VIIRS and AMSR2. *J. Atmos. Oceanic Technol.*, **33**, 361–375, https://doi.org/10.1175/JTECH-D-15-0093.1.

Castro, S. L., G. A. Wick, and M. Steele, 2016: Validation of satellite sea surface temperature analyses in the Beaufort Sea using UpTempO buoys. *Remote Sens. Environ.*, **187**, 458–475, https://doi.org/10.1016/j.rse.2016.10.035.

Cavalieri, D. J., C. L. Parkinson, P. Gloersen, and H. J. Zwally, 1996: Sea ice concentrations from Nimbus-7 SMMR and DMSP SSM/I-SSMIS passive microwave data, version 1. NASA National Snow and Ice Data Center Distributed Archive Center. Subset used: 2011–17, accessed March 2018, https://doi.org/10.5067/8GQ8LZQVL0VL.

——, ——, ——, J. C. Comiso, and H. J. Zwally, 1999: Deriving long-term time series of sea ice cover from satellite passive-microwave multisensory data sets. *J. Geophys. Res.*, **104**, 15 803–15 814, https://doi.org/10.1029/1999JC900081.

Chin, T. M., J. Vazquez-Cuervo, and E. M. Armstrong, 2017: A multi-scale high-resolution analysis of global sea surface temperature. *Remote Sens. Environ.*, **200**, 154–169, https://doi.org/10.1016/j.rse.2017.07.029.

Donlon, C. J., M. Martin, J. Stark, J. Roberts-Jones, E. Fiedler, and W. Wimmer, 2012: The Operational Sea Surface Temperature and Sea Ice Analysis (OSTIA) system. *Remote Sens. Environ.*, **116**, 140–158, https://doi.org/10.1016/j.rse.2010.10.017.

Fofonoff, N. P., and R. C. Millard, 1983: Algorithms for computation of fundamental properties of seawater. UNESCO Tech. Paper in Marine Science 44, 53 pp.

Grumbine, R. W., 2014: Automated sea ice concentration analysis history at NCEP: 1996–2012. NOAA Modeling Branch Tech. Note 321, 39 pp., https://polar.ncep.noaa.gov/mmab/papers/tn321/MMAB_321.pdf.

Hurrell, J. W., J. J. Hack, D. Shea, J. M. Caron, and J. Rosinski, 2008: A new sea surface temperature and sea ice boundary dataset for the Community Atmosphere Model. *J. Climate*, **21**, 5145–5153, https://doi.org/10.1175/2008JCLI2292.1.

Lavelle, J., R. Tonboe, M. B. Jensen, and E. Howe, 2017: Validation report for OSI SAF global sea ice concentration: Product OSI-401-b—Version 1.2. EUMETSAT Rep., 27 pp., http://osisaf.met.no/docs/osisaf_cdop3_ss2_valrep_ice-conc_v1p2.pdf.

Levitus, S., 1982: *Climatological Atlas of the World Ocean*. NOAA Professional Paper 13, U.S. Dept. of Commerce, 173 pp.

Maturi, E., A. Harris, J. Mittaz, J. Sapper, G. Wick, X. Zhu, P. Dash, and P. Koner, 2017: A new high-resolution sea surface temperature blended analysis. *Bull. Amer. Meteor. Soc.*, **98**, 1015–1026, https://doi.org/10.1175/BAMS-D-15-00002.1.

Rayner, N. A., D. E. Parker, E. B. Horton, C. K. Folland, L. V. Alexander, D. P. Rowell, E. C. Kent, and A. Kaplan, 2003: Global analyses of sea surface temperature, sea ice, and night marine air temperature since the late nineteenth century. *J. Geophys. Res.*, **108**, 4407, https://doi.org/10.1029/2002JD002670.

Reynolds, R. W., N. A. Rayner, T. M. Smith, D. C. Stokes, and W. Wang, 2002: An improved in situ and satellite SST analysis for climate. *J. Climate*, **15**, 1609–1625, https://doi.org/10.1175/1520-0442(2002)015<1609:AIISAS>2.0.CO;2.

——, T. M. Smith, C. Liu, D. B. Chelton, K. S. Casey, and M. G. Schlax, 2007: Daily high-resolution-blended analyses for sea surface temperature. *J. Climate*, **20**, 5473–5496, https://doi.org/10.1175/2007JCLI1824.1.

Steele, M., W. Ermold, and I. Rigor, 2018: UpTempO buoys deployed in the Arctic Ocean in 2017. Arctic Data Center, accessed 20 November 2018, https://doi.org/10.18739/A2GB1XG6P.

Strong, C., and K. Golden, 2016: Filling the polar data gap in sea ice concentration fields using partial differential equations. *Remote Sens.*, **8**, 442, https://doi.org/10.3390/rs8060442.

Thiebaux, J. E., 2003: A new high-resolution blended real-time global sea surface temperature analysis. *Bull. Amer. Meteor. Soc.*, **84**, 645–656, https://doi.org/10.1175/BAMS-84-5-645.

Zweng, M. M., and Coauthors, 2013: *Salinity*. Vol. 2, *World Ocean Atlas 2013*, NOAA Atlas NESDIS 74, 39 pp., http://data.nodc.noaa.gov/woa/WOA13/DOC/woa13_vol2.pdf.